Ministry of Science, Research & Technology
Iranian Research Organization for Science and Technology

Journal of PARTICLE Science & Technology

JPSIT

https://jpst.irost.ir

Research paper

Synthesis and characterization of the aminated nano-zeolite: A green heterogeneous nanocatalyst for the synthesis of valuable organic compounds

Khadijeh Rabiei* **and Fatemeh Najafi**

[1] *Department of Chemistry, Qom University of Technology, Qom, Iran*

HIGHLIGHTS

- Synthesis of green heterogeneous nanocatalyst.
- Functionalization of nano-clinoptilolite.
- Synthesis of valuable organic compounds.
- Excellent yields and short reaction times.

GRAPHICAL ABSTRACT

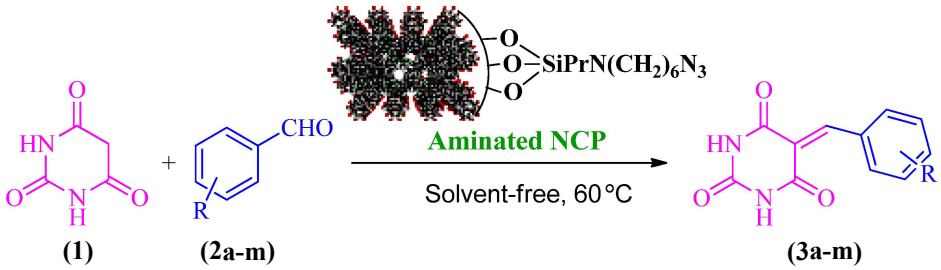

ARTICLE INFO

Article history:

Received 14 November 2022
Revised 24 December 2022
Accepted 29 December 2022

Keywords:

$NCP@SiO_3Pr(CH_2)_6N_4$
α,β-Unsaturated compounds
Clinoptilolite
Green nanocatalyst
Barbituric acid

ABSTRACT

In this study, natural surface-modified nano-clinoptilolite, $NCP@SiO_3Pr(CH_2)_6N_4$, was synthesized and fully characterized using various analytical techniques, including FT-IR, XRD, SEM, EDS, TEM, and TG-DTA analyses. Additionally, this aminated nanocatalyst was evaluated for the effective synthesis of *α,β*-unsaturated carbonyl compounds containing valuable substances such as barbituric acid moiety under solvent-free conditions. This catalyst obtained desired products with excellent yields, high purity, and short reaction times. Furthermore, the synthetic, non-toxic heterogeneous nanocatalyst is easily recycled and can be reused several times.

* *Corresponding author: Tel.: +9825-36641601 ; Fax: +9825-36641601 ; E-mail address: rabiei@qut.ac.ir*
DOI: 10.22104/JPST.2023.5964.1217

1. Introduction

The development of green and clean transformations to synthesize pharmaceutical compounds is a challenge facing chemists today [1,2]. Developing heterogeneous catalysts using renewable materials, non-toxic chemicals, heterogeneous catalysts, and solvent-free conditions are fundamental issues in the green synthetic strategy. Solid-supported heterogeneous catalysts are considered green media and have received significant attention in organic synthesis. These catalysts have unique advantages, including high stability, simple work-up procedures, efficiency, reusability, and low toxicity [3-7].

Various materials such as clay, silica, zeolite, metal oxide, and other mesoporous materials have been utilized as solid supports [8,9]. However, with good thermal stability and large surface area, natural zeolite clinoptilolite has been utilized in various industrial and synthetic fields [10]. Moreover, convenient surface modification by different chemical reagents is a unique advantage of zeolite clinoptilolite [11-13]. Recently, as heterogeneous catalysts or ideal supports for homogeneous catalysts, zeolites have been offered as an effective green medium for organic reactions [14,15].

Chalcones (*α*,*β*-unsaturated Michael acceptors) are naturally abundant or synthetic compounds with a broad spectrum of pharmaceutical activities, including antimalarial [16,17], antihyperglycemic [18], antibacterial [19], antidiabetic [20] and antitumor [21]. Chalcones, or 1,3-diaryl/heteroaryl-2-propene-1-ones, are an attractive molecular scaffold that have been widely used as starting or intermediate material to synthesize various bioactive heterocycles [22-24].

On the other hand, barbituric acid and its derivatives have recently attracted significant attention because of their versatile biological properties, including sedatives, hypnotic, cardiovascular, anticonvulsants, inhibitors of metal corrosion, *etc.* [25]. According to previous studies, many synthetic drugs bear a barbituric acid core. Also, 2-Arylidenindane-1,3-diones are an important class of chemicals that have various applications in medical science and industrial fields. Some of these *α*,*β*-unsaturated carbonyl compounds show antibacterial, anticoagulant, nonlinear optical, and electroluminescent properties [26-28]. Various methods using different catalysts have been used to synthesize these compounds [29-31].

From the viewpoint of diversity and the importance of green chemistry, it is crucial to design and develop new and green synthetic methods for constructing *α*,*β*-unsaturated Michael acceptor derivatives.

In our ongoing research on the green synthesis of various compounds [32,33], a novel and efficient approach for the synthesis of *α*,*β*-unsaturated Michael acceptor derivatives using an eco-friendly, reusable, functionalized nano heterogeneous catalyst was developed in this study.

2. Experimental

2.1. Materials and apparatus

The desired materials were purchased from the Merck company and used without any purification. The zeolite was obtained from the Semnan mine. Melting points were determined using an Electrothermal MK3 apparatus. ^{1}H-NMR and ^{13}C-NMR were recorded on a Bruker DRX-400 spectrometer in DMSO solvent with tetramethylsilane as the internal reference. FT-IR spectra were determined using a Perkin-Elmer FT-IR 550 Spectrometer. A TEM image was obtained using a TEM Philips EM 208S instrument. The XRD patterns were obtained by an XPertHigh Score (PW1800) instrument with 1.54 A. High Score Plus and Digimizer software were used to carry out the calculations related to the crystallite size and its distribution. The EDS and SEM images of nanocatalysts were recorded on an FE-SEM MIRA3 TESCA instrument. The TG-DTA analysis was recorded for the samples using the STA 503 model in a 25 - 900 °C range with a temperature rise of 10 °C.min^{-1} under argon atmosphere. Also, the purity of the substrates and reaction progress were checked by TLC on silica-gel Polygram SILG/UV 254 plates.

2.2. Preparation of NCP@SiO$_3$PrCl

3-ClPrSi(OMe)$_3$ (1.5 ml) was added to a mixture of NCP (**A**) (1.5 g) in $CHCl_3$ (5 ml) under constant stirring (5 h) at room temperature. After the reaction was completed, the NCP@SiO$_3$PrCl was separated by filtration, washed with CH_2Cl_2 (2×4 ml), and dried in an oven at 80 °C temperature.

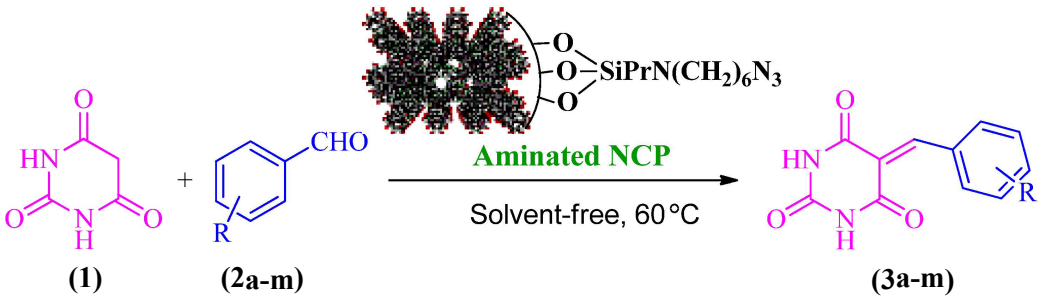

Fig. 1. Synthesis of various *α,β*-unsaturated carbonyl compounds in the presence of an aminated nanocatalyst.

2.3. Preparation of aminated nano-clinoptilolite (NCP@SiO$_3$PrN(CH$_2$)$_6$N$_3$)

The synthetic NCP@SiO$_3$PrCl (**B**) (1 g) was first poured into a round bottom flask equipped with a magnetic stirrer, and $CHCl_3$ (10 ml) was added to it. The mixture was stirred for 15 min at room temperature. Then HMTA (1.4 g) was added dropwise to the reaction mixture and stirred for 4 h under reflux conditions. When we were sure the reaction was completed, the mixture was filtered, washed with CH_2Cl_2 (3×5 ml), and dried in an oven under 90 °C [33].

*2.4. General procedure for the synthesis of α,β-unsaturated (**3a-m**) compounds*

A mixture of barbituric acid (1 mmol) and aromatic aldehyde (1 mmol) was poured into a 25 ml round bottom flask, and synthetic NCP@SiO$_3$PrHMTA (0.006 g) was added to the mixture and stirred for an appropriate time (5-12 min) at 60 °C. The progress of the reaction was followed by TLC (EtOAc/Hexane, 2/10). After the reaction completion (checked by TLC), the precipitated solid was washed twice with $CHCl_3$ (4 ml) to remove the catalyst, which can be used in the subsequent reaction. The filtrate was concentrated, and the crude product was finally purified by recrystallization from EtOH. The desired *α,β*-unsaturated compounds were obtained with excellent yields of 94-98% after short reaction times (5-12 min) using the green and basic nanocatalyst NCP@SiO$_3$PrHMTA (**C**) (Fig. 1). The structure of synthetic products was identified by spectroscopic data, as shown in Table 1.

3. Results and discussion

3.1. Preparation and characterization of functionalized aminated nano-zeolite clinoptilolite (NCP@SiO$_3$Pr(CH$_2$)$_6$N$_4$)

A general pathway for the synthesis of NCP@SiO$_3$Pr(CH$_2$)$_6$N$_4$ nano-clinoptilolite as a low-cost, non-toxic, reusable, heterogeneous nanocatalyst is depicted in Fig. 2, in accordance with our previous report [33]. In the first step, nano-clinoptilolite was obtained from bulk zeolite clinoptilolite through a green mechanical method using a ball mill. In the

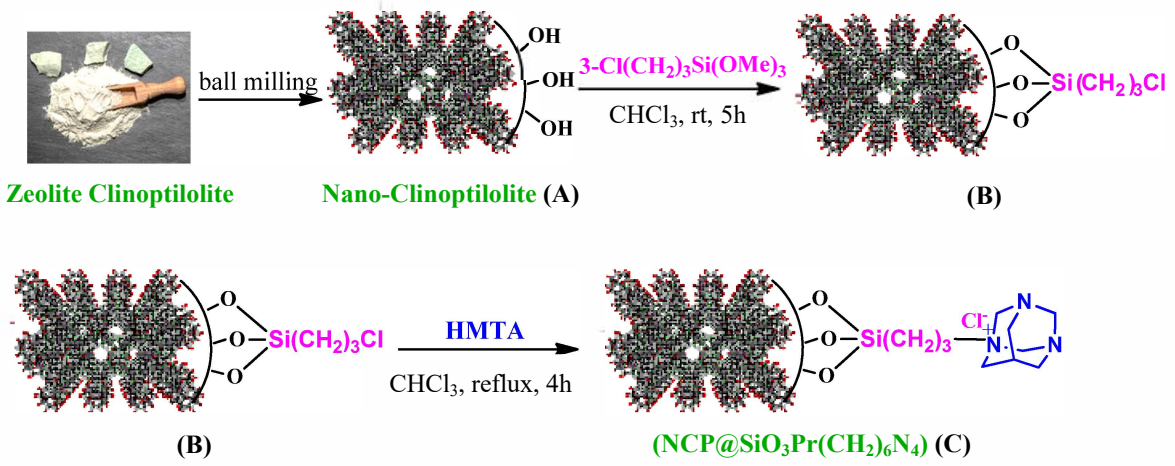

Fig. 2. The simplified schematic representation for the preparation of aminated nano-clinoptilolite (**C**).

Table 1. The spectroscopic data of products (**3a-m**).

Product	FT-IR (KBr) (cm^{-1})	^{1}H-NMR (400 MHz, DMSO-d_6) (δ, ppm)	^{13}C-NMR (100 MHz, DMSO-d_6) (δ, ppm) and Anal. Calcd. (CHN)
5-(phenylmethylidene)-1,3-diazinane-2,4,6-trione (**3a**)	3455 (br, NH), 3215 (CH, sp^2), 1746 (C=O), 1570 (C=C), 1443, 1403 (C=C, Ar)	7.45-8.09 (m, 5H, Ar), 8.28 (s, 1H, CH), 11.24 (s, 1H, NH), 11.40 (s, 1H, NH)	119.33, 128.27, 132.43, 132.90, 133.33, 150.44, 154.95, 161.80, 163.63
5-[(4-Chlorophenyl) methylidene]-1,3-diazinane-2,4,6-trione (**3b**)	3435 (br, NH), 3209 (CH, sp^2), 1738 (C=O), 1570 (C=C), 1440, 1498 (C=C, Ar)	7.52-7.54 (d, J=8 Hz, 2H, Ar), 8.06-8.08 (d, J=8 Hz, 2H, Ar), 8.24 (s, 1H, CH), 11.27 (s, 1H, NH), 11.42 (s, 1H, NH)	120.37, 128.29, 128.84,130.12, 131.94, 132.30, 135.43, 137.51, 150.94, 153.85, 162.33, 163.97, 192.91
5-[(4-methylphenyl) methylidene]-1,3-diazinane-2,4,6-trione (**3c**)	3441 (br,NH), 3038 (CH sp^2), 1726 (C=O), 1655 (C=C), 1490,1540 (C=C, Ar)	2.38 (s, 3H, CH_3), 7.29-7.31 (d, J=8Hz, 2H, Ar), 8.08-8.10 (d, J=8Hz, 2H, Ar), 8.25 (s, 1H, CH), 11.21 (S, 1H, NH), 11.35 (s, 1H, NH)	117.87, 128.86, 129.87, 133.97, 143.46, 150.21, 154.95, 161.80, 163.60
5-[(4-methoxyphenyl) methylidene]-1,3-diazinane-2,4,6-trione (**3d**)	3211 (br, NH), 3074 (CH sp^2), 1741 (C=O), 1550 (C=C), 1460, 1398 (C=C, Ar)	3.87 (s, 3H, OCH_3), 7.05-7.07 (d, J=8Hz, 2H, Ar), 8.25 (s, 1H, CH), 8.36-8.38 (d, J=8Hz, 2H, Ar), 11.17 (s, 1H, NH), 11.30 (s, 1H, NH)	55.70, 113.95, 115.53, 125.18, 137.52, 150.23, 155.01, 162.19, 163.47, 163.94.
5-[(4-nitrophenyl) methylidene]-1,3-diazinane-2,4,6-trione (**3e**)	3429 (br, NH), 3098 (CH sp^2), 1688 (C=O), 1595 (C=C), 1516, 1440 (C=C, Ar)	8.01-8.03 (d, J=8Hz, 2H, Ar), 8.24-8.26 (d, J=8Hz, 2H, Ar), 8.33 (s, 1H, CH), 11.33 (s, 1H, NH), 11.50 (s, 1H, NH)	122.33, 122.72, 124.30, 130.96, 132.33, 140.03, 148.08, 150.26, 151.25, 161.21, 162.71, 192.35
5-{[4-(dimethylamino)phenyl] methylidene}-1,3-diazinane-2,4,6-trione (**3f**)	3445 (br, NH), 3034 (CH sp^2), 1725 (C=O), 1654 (C=C), 1494,1445 (C=C, Ar),	3.11 (s, 3H, CH_3), 3.37 (s, 3H, CH_3), 6.77-6.79 (d, J=8Hz, 2H, Ar), 8.14 (s, 1H, CH), 8.40-8.42 (d, J=8Hz, 2H, Ar), 10.92 (s, 1H,NH), 11.05 (s, 1H, NH)	39.16, 39.87, 109.73, 111.38, 120.20, 139.26, 150.52, 154.34, 155.96, 162.92, 164.91
5-(2-oxo-2,3-dihydro-1H-indol-3-ylidene)-1,3-diazinane-2,4,6-trione (**3g**)	3362 (br,NH), 3099 (CH sp^2), 1712 (C=O), 1650 (C=C), 1417, 1337 (C=C, Ar)	5.04 (s, 1H, NH), 6.67-7.13 (m, 4H, Ar), 10.57 (s, 1H, NH), 11.19 (s, 1H, NH)	109.51, 112.27, 121.52, 122.84, 124.33, 124.74, 128.15, 128.85,138.45, 143.23, 150.29, 167.83, 175.73
5-[(2,4-dimethylphenyl) methylidene]-1,3-diazinane-2,4,6-trione (**3h**)	3439 (br, NH), 3086 (CH sp^2), 1674 (C=O), 1580 (C=C), 1435, 1383 (C=C, Ar)	2.28 (s, 3H, CH_3), 2.31 (s, 3H, CH_3), 7.00-7.03 (d, J=8Hz, 1H, Ar), 7.10 (s, 1H, Ar), 7.62-7.64 (d, J=8Hz, 1H, Ar), 8.39 (s, 1H, CH), 11.15 (s, 1H, NH), 11.37 (s, 1H, NH)	119.31, 125.63, 129.86, 130.36, 130.74, 138.48, 141.13, 150.29, 153.57, 161.24, 163.26; Anal. Calcd. For $C_{13}H_{12}N_2O_3$: C, 63.93; H, 4.95; N, 11.47, Found: C, 64.35; H, 5.05; N, 11.47
5-[(3-chlorophenyl) methylidene]-1,3-diazinane-2,4,6-trione (**3i**)	3522 (br, NH), 3035 (CH sp^2), 1694 (C=O), 1611 (C=C), 1463, 1404 (C=C, Ar)	7.47-8.17 (m, 4H, Ar), 8.24 (s, 1H, CH), 11.23 (s, 1H, NH), 11.44 (s, 1H, NH)	Anal. Calcd. For $C_{11}H_7ClN_2O_3$: C, 52.71; H, 2.82; N, 11.18; Found: C, 52.98; H, 2.92; N, 11.18
5-[(3-methoxyphenyl) methylidene]1,3-diazinane-2,4,6-trione (**3j**)	3240 (br, NH), 3084 (CH sp^2), 1740 (C=O), 1550 (C=C), 1450, 1398 (C=C, Ar)	3.79 (s, 3H, OCH_3), 7.11-7.85 (m, 4H, Ar), 8.26 (s, 1H, CH), 11.25 (s, 1H, NH), 11.40 (s, 1H, NH)	Anal. Calcd. For $C_{12}H_{10}N_2O_4$: C, 58.54; H, 4.09; N, 11.38, Found: C, 58.84; H, 4.19; N, 11.34
5-[(2-chlorophenyl) methylidene]-1,3-diazinane-2,4,6-trione (**3l**)	3428 (br, NH), 3080 (CH sp^2), 1690 (C=O), 1610 (C=C), 1463, 1404 (C=C, Ar)	7.35-7.76 (m, 4H, Ar), 8.29 (s, 1H, CH), 11.26 (s, 1H, NH), 11.48 (s, 1H, NH)	123, 126, 127, 128, 129, 133, 135, 145, 153, 187, 189; Anal. Calcd. For $C_{11}H_7ClN_2O_3$: C, 52.71; H, 2.82; N, 11.18; Found: C, 53.01; H, 2.95; N, 11.19
5-[(2-nitrophenyl) methylidene]-1,3-diazinane-2,4,6-trione (**3m**)	3237 (br, NH), 3082 (CH sp^2), 1684 (C=O), 1599 (C=C), 1517, 1439 (C=C, Ar)	7.56-8.24 (m, 4H, Ar), 8.61 (s, 1H, CH), 11.25 (s, 1H, NH), 11.50 (s, 1H, NH)	122, 127, 128, 129, 132, 133, 1469, 157, 188, 189

second step, the reaction of nano-clinoptilolite and 3-chloropropyl trimethoxysilan was investigated for the synthesis of the desired functionalized NCP@SiO_3PrCl. In continuation of the NCP modifying process, the nano-clinoptilolite NCP (**C**) was prepared through the nucleophilic substituted reaction of the Cl atom on the NCP (**B**) surface, with the nitrogen of hexamethylenetetramine (HMTA) under reflux conditions [33]. The structure of the synthetic NCP@$SiO_3Pr(CH_2)_6N_4$ was characterized using various analytical techniques such as FT-IR, XRD, FE-SEM, EDS, TEM, and TG-DTA analyses (Supplementary File).

In FT-IR spectra (Fig. S1), the functional groups' existence was confirmed by comparing the FT-IR spectra of NCP (**A**) with NCPs (**C**). In Fig. S1(a), symmetric and asymmetric stretching vibration at wave number 3452 cm^{-1} contributed to the hydrogen bonding of the H_2O molecules to surface oxygen, and the medium intensity band (1640 cm^{-1}) attributed to the bending H–O–H vibration. The tetrahedral-octahedral, (T-O), stretching vibration of the Si–O, Si–O–Al, and Al–O bonds appeared at 1077 cm^{-1}. The next vibration, at 462 cm^{-1}, is assigned to a T-O bending of O–Si–O and O–Al–O [33].

The FT-IR spectra of NCP@$SiO_3Pr(CH_2)_6N_4$ (**C**) is presented in Fig. S1(b). The asymmetric stretching vibration of the hydroxyl group linked on the nano-zeolite clinoptilolite surface appeared as a broad band at 3450 cm^{-1}, and the bending H–O–H vibration appeared at wave number 1634 cm^{-1}. Also, two bands at 2873 and 2941 cm^{-1} were attributed to the C–H group. The band at 1237 cm^{-1} was assigned to the stretching vibration of C–N. All of these observations confirmed the modification of the nano-clinoptilolite surface.

Using scanning electron microscopy (SEM) and transition electron microscopy (TEM), the morphology of functionalized nano-clinoptilolite (**C**) and pure nano-clinoptilolite (**A**) was examined (Figs. S2 and S3). Additionally, the particle distribution was calculated using the NCP (**C**) SEM image (Fig. S4)

The X-ray diffraction analyses of nano-clinoptilolites (**A**) and (**C**) are indicated in Fig. S5. The intense peak at $2\theta = 26.60°$ was assigned to *d*-spacing values of 3.35 Å. It is clear from the similarities in XRD patterns of NCP (**A**) and (**C**) that chemical attachment to nano-clinoptilolite was only affected its surface without destroying the NCP's original structure. In Fig. S5, the peak at $2\theta = 17.95°$ is related to the existence of hexamethylene tetraamine linked on the nano-zeolite clinoptilolite surface [40]. The crystallite size of the NCP (**C**) was calculated using the Scherrer Equation (see Fig. S6). As shown in this figure, the average crystallite size of NCP (**C**) was 35 nm.

Analysing the NCP with EDX technique, confirmed the formation of functionalized nano-clinoptilolite (**C**). The results of the elemental analysis of NCP (**A**) and NCP (**C**) are shown in Fig. S7. The existence of C and N elements in the EDX analysis (Fig. S7) agrees with the NCP@$SiO_3PrN(CH_2)_6N_3$ (**C**) structure.

Thermal gravimetrical analysis (TGA) was performed to characterize the functionalized nano-clinoptilolite further. TG analysis of the nano-zeolite clinoptilolite (**A**) and (**C**) are presented in Fig. S8. As seen in the figure, the loading of the desired functional group was confirmed by comparing the TGA diagram of modified nano-clinoptilolite (**C**) with the TGA curve of nano-clinoptilolite (**A**). The TGA of NCP (**C**) shows that the initial weight loss that occurs up to 200 °C is associated with water desorption, the approximate 32 % weight loss occurring between 200 to 260 °C corresponds to the linked group decomposition, and the 12 % weight loss between 260 to 800 °C is related to the observed elimination of water. In the DTA diagram of the modified NCP (**C**), an exothermal signal was observed in the range of 200 - 260 °C, which agrees with the elimination of organic compounds loaded on the nano-clinoptilolite surface. Also, it seems that the endothermal signal in the range of 260 - 500 °C is related to the elimination of water molecules. All of the mentioned figures are indicated in the Supplementary File.

To continue the previous investigation of the catalytic efficiency of this synthetic aminated nano heterogeneous catalyst, the preparation of valuable *α,β*-unsaturated carbonyl compounds was studied in the presence of synthesized NCP@$SiO_3Pr(CH_2)_6N_4$.

*3.2. Survey of the synthesis of α,β-unsaturated carbonyl compounds in the presence of NCP@$SiO_3Pr(CH_2)_6N_4$ (**C**)*

In continuation of the successful synthesis of novel basic functionalized nanoclinoptilolite and survey catalytic efficiency for the preparation of Mannich bases [33], we focused our attention on the utility of the novel synthetic basic functionalized nano-clinoptilolite for

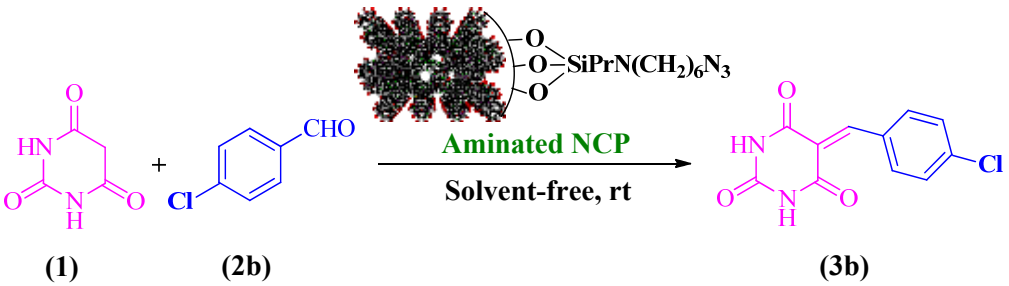

Fig. 3. Preparation of the compound (**3b**) in the presence of the aminated NCP under solvent-free conditions.

the preparation of *α,β*-unsaturated carbonyl compounds including arylidene barbituric acid. For this purpose, the condensation reaction of 4-chlorobenzaldehyde with barbituric acid was chosen as the model reaction (Fig. 3). Due to the optimization of this reaction, the influence of various amounts of synthetic nanocatalyst NCP@$SiO_3Pr(CH_2)_6N_4$ and different temperatures were examined under solvent-free conditions. The results are summarized in Tables 2 and 3.

As seen in Table 2, the desired product (**3b**) was obtained in a good yield when 0.006 g of NCP (**C**) was used (entry 6 in Table 2). There was no product observed in the absence of the catalyst.

Table 3 represents the results of our investigation of temperature effects. At 60 ºC under solvent-free conditions, entry 3 showed excellent yield and short reaction time of desired *α,β*-unsaturated carbonyl compound (**3b**). It is also worth mentioning that increasing the temperature up to 140 °C did not affect the progress of product yield (Table 3, entry 6).

A general study of this protocol was carried out using various aromatic aldehydes and ketones containing electron-donating and electron-withdrawing groups in conjunction with barbituric acid for the synthesis of *α,β*-unsaturated carbonyl compounds (**3a-m**) under optimal conditions. As is observable, by using this novel, green and basic nanocatalyst, NCP@$SiO_3PrN(CH_2)_6N_3$ (**C**), the aromatic aldehydes containing both electron-donating and electron-withdrawing groups afforded the corresponding products (**3a-m**) with excellent yields and short reaction times (Table 4). The structure of the synthetic products was characterized by various spectroscopic data.

Table 2. Optimization of catalyst amount for the synthesis of (**3b**) under solvent-free conditions.

Entry	Amount of catalyst (g)	Time (min)	Yield[a] (%)
1	-	90	No product
2	0.001	15	35
3	0.002	15	45
4	0.003	15	60
5	0.004	15	75
6	0.006	15	90
7	0.007	15	90
8	0.008	15	90
9	0.009	15	90
10	0.02	15	90

[a] Isolated yield

*3.3. Mechanism of formation for the α,β-unsaturated carbonyl compounds (**3a**) using NCP@ $SiO_3PrN(CH_2)_6N_3$ (**C**)*

The proposed mechanism for the preparation of *α,β*-unsaturated carbonyl compounds containing valuable barbituric acid moiety in the presence of the heterogeneous nanocatalyst (**C**) is displayed in Fig 4.

*3.4. Determination of the synthetic nanocatalyst NCP (**C**) reusability*

In accordance with green chemistry rules and the importance of the reusability of heterogeneous catalysts,

Table 3. Optimization of temperature effect for preparation of (**3b**) in the presence of NCP (**C**) (0.006 g) under solvent-free conditions.

Entry	Temperature (°C)	Time (min)	Yield[a] (%)
1	rt	15	90
2	50	12	93
3	60	9	97
4	70	9	97
5	100	8	97
6	140	6	97

[a] Isolated yield

Table 4. Green synthesis of compounds (**3a-m**) from barbituric acid and substrates (**2a-m**) in the presence of NCP@$SiO_3PrN(CH_2)_6N_3$ (**C**) as an efficient nanocatalyst.

Entry	Substrate (2)	Product	Time (min)	Yield[a] (%)
1	**2a**	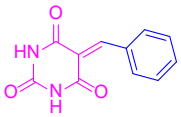	10	95
2	**2b**	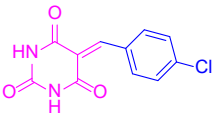	9	97
3	**2c**	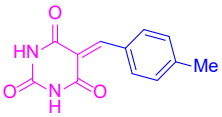	10	95
4	**2d**	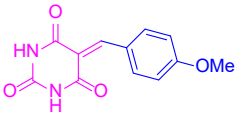	12	97
5	**2e**	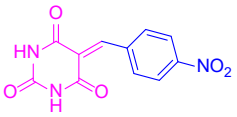	5	98
6	**2f**	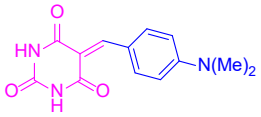	7	96
7	**2g**	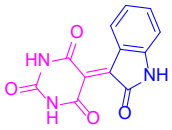	6	97
8	**2h**	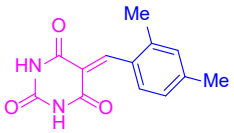	8	94
9	**2i**	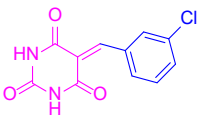	7	97
10	**2j**	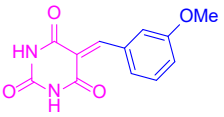	8	97
11	**2k**	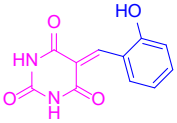	10	96
12	**2l**	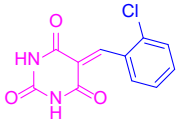	7	97
13	**2m**	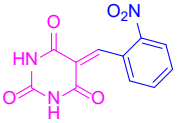	6	97

[a] Isolated yield

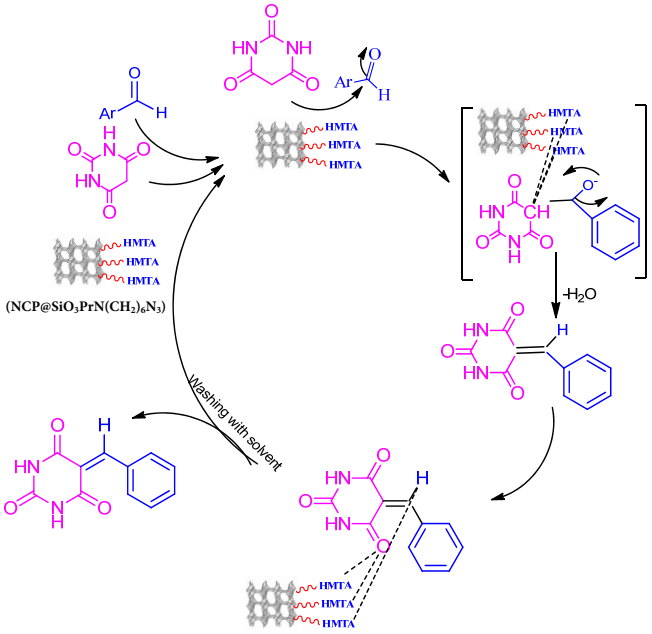

Fig. 4. The proposed mechanism for the synthesis of α,β-unsaturated carbonyl compounds using modified nano-clinoptilolite (MNCP) catalyst.

the recycling of this synthetically modified nanocatalyst was studied in a reaction model to synthesize the corresponding product (**3a**). After the workup of the product (**3a**), the catalyst was washed with CH_2Cl_2 (6 ml), dried at 90 °C in an oven for 8 h, and reused in the next reaction. The results are summarized in Fig. 5. This figure shows that the synthetic nanocatalyst was reused in the same response for at least six consecutive runs with remarkable activity retention.

In addition, the efficiency of this novel method using a heterogeneous nanocatalyst for the preparation of the corresponding α,β-unsaturated carbonyl compounds (**3a-m**) was compared with other reported catalytic methods. The results are shown in Table 5.

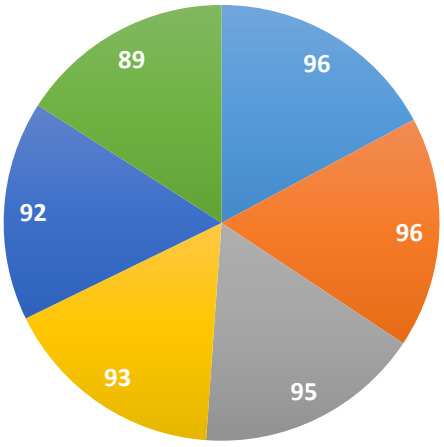

Fig. 5. Reusability of the modified nanocatalyst (**C**).

Table 5. Comparison of catalytic efficiency of NCP@SiO_3PrHMTA with other reported methods for the synthesis of compound (**3b**).

Entry	Catalyst, Conditions	Time (min)	Ref.	Yield (%)
1	BF_3/nano-γ-Al_2O_3/Ethanol, RT	30	[41]	84
2	Aminosulfonic acid / Grinding	180	[42]	96
3	[bmim]BF_4 / Grinding-laying	120	[43]	78
4	$Ce_1Mg_xZr_{1-x}O_2$ (CMZO) / MW	3	[44]	94
5	[H-Suc]HSO_4	7	[45]	94
6	NCP@SiO_3PrHMTA, 60 °C	9	This work	97
7	NCP, 60 °C	90	-	55

4. Conclusion

In conclusion, we have reported the synthesis of a green and efficient nano heterogeneous natural basic catalyst through the modification of the nano-zeolite clinoptilolite surface using the reaction of the synthetic nano-zeolite clinoptilolite with chlolropropyl trimethoxysilan and HMTA reagents. The structure of the modified nano-zeolite was characterized using various techniques, including FT-IR, XRD, SEM, TEM, EDS, and TG-DTA analyses. Then, the catalytic activity of this nanocatalyst was studied for the green synthesis of *α*,*β*-unsaturated carbonyl compounds containing barbituric acid moiety (**3a-m**) under solvent-free conditions. Using this nanocatalyst resulted in the desired products in excellent yields and short reaction times by easy workup. The catalyst was reused in at least six consecutive runs with remarkable activity retention.

Acknowledgments

The authors express appreciation to the Qom University of Technology for supporting this investigation.

Disclosure Statement

No potential conflict of interest was reported by the authors.

References

[1] Sathishkumar, M., Nagarajan, S., Shanmugavelan, P., Dinesh, M., & Ponnuswamy, A. (2013). One-pot regio/stereoselective synthesis of 2-iminothiazolidin-4-ones under solvent/scavenger-free conditions. *Beilstein J. Org. Chem. 9*(1) 689-697.

[2] Manujyothi, R., Aneeja, T., & Anilkumar, G. (2021). Solvent-free synthesis of propargylamines: An overview. *RSC Adv.* 11, 19433-19449.

[3] Ghezali, S., Mahdad-Benzerdjeb A., Ameri M., & Bouyakoub, A.Z. (2018). Adsorption of 2,4,6-trichlorophenol on bentonite modified with benzyl dimethyltetradecylammonium chloride. *Chem. Int. 4*(1) 24-32.

[4] Naeimi, H., and Nazifi, Z.S. (2014). Sulfonated diatomite as heterogeneous acidic nanoporous catalyst for synthesis of 14-aryl-14-*H*-dibenzo[*a*,*j*] xanthenes under green conditions. *Appl. Catal. A.-Gen.* 477, 132-140.

[5] Sivaguru, P., and Lalitha, A. (2014). Ceric ammonium nitrate supported HY-zeolite: An efficient catalyst for the synthesis of 1,8-dioxooctahydroxanthenes. *Chinese Chem. Lett. 25*(2) 321-323.

[6] Li, P., Regati, S., Huang, H.C., Arman, H.D., Chen, B.L., & Zhao, J.C.G. (2015). A sulfonate-based Cu(I) metal-organic framework as a highly efficient and reusable catalyst for the synthesis of propargylamines under solvent-free conditions. *Chinese Chem. Lett. 26*(1) 6-10.

[7] Jetti, S. R., Bhatewara, A., Kadre, T., & Jain, S. (2014). Silica-bonded N-propyl sulfamic acid as an efficient recyclable catalyst for the synthesis of 3,4-dihydropyrimidin-2-(1*H*)-ones / thiones under heterogeneous conditions. *Chinese Chem. Lett. 25*(3) 469-473.

[8] Kalhor, M., and Zarnegar, Z. (2019). Fe_3O_4/SO_3H@ Zeolite-Y as a novel multi-functional and magnetic nanocatalyst for clean and soft synthesis of imidazole and perimidine derivatives. *RSC Adv. 9*, 19333-19347.

[9] Tamiji, T., and Nezamzadeh-Ejhieh, A. (2019). Sensitive voltammetric determination of bromate by using ion-exchange property of a Sn(II)-clinoptilolite-modified carbon paste electrode. *J. Solid State Electr.* 23, 143-157.

[10] Miądlicki, P., Wróblewska, A., Kiełbasa, K., Koren, Z.C., & Michalkiewicz, B. (2021). Sulfuric acid modified clinoptilolite as a solid green catalyst for solvent-free α-pinene isomerization process. *Micropor. Mesopor. Mat.* 324, 111266-111280.

[11] Markovi, M., Dakovi, A., Rottinghaus, G.E., Kragovi, M., Petkovi, A., Krajišnik, D., Mili, J.,

Mercurio, M., & Gennaro, B. (2017). Adsorption of the mycotoxin zearalenone by clinoptilolite and phillipsite zeolites treated with cetylpyridinium surfactant. *Colloid. Surface. B.* 151, 324-332.

[12] Zhao, Y., Zhao, X., Deng, J., & He, C. (2016). Uilization of chitosan–clinoptilolite composite for the removal of radiocobalt from aqueous solution: Kinetics and thermodynamics. *J. Radioanal. Nucl. Chem.* 308, 701-709.

[13] Yener, H.B., Yılmaz, M., Deliismail, O., Ozkan, S.F., Helvac, S.S. (2017). Clinoptilolite supported rutile TiO_2 composites: Synthesis, characterization, and photocatalytic activity on the degradation of terephthalic acid. *Sep. Purif. Technol.* 173, 17-26.

[14] Baghbanian, S.M. (2015). Propylsulfonic acid functionalized nano-zeolite clinoptilolite as heterogeneous catalyst for the synthesis of quinoxaline derivatives. *Chinese Chem. Lett. 26*(9) 1113-1116.

[15] Guzel, P., Aydın, Y.A., & Deveci Aksoy, N. (2016). Removal of chromate from wastewater using amine-based-surfactant-modified clinoptilolite. *Int. J. Environ. Sci .Te.* 13, 1277-1288.

[16] Elkanzi, N.A.A., Hrichi, H., Alolayan, R.A., Derafa, W., Zahou, F.M., & Bakr, R.B. (2022). Synthesis of chalcones derivatives and their biological activities: A review. *ACS Omega*, *7*(32) 27769-27786.

[17] Aljohani, G., Al-Sheikh Ali, A., Alraqa, S.Y., Amran, S., & Basar, N. (2021). Synthesis, molecular docking and biochemical analysis of aminoalkylated naphthalene-based chalcones as acetylcholinesterase inhibitors. *J. Taibah Univ. Sci. 15*(1) 781-797.

[18] Jain, A., and Jain, D. (2019). Synthesis, characterization and biological evaluation of some new heterocyclic derivatives of chalcone as antihyperglycemic agents. *Int. J. Pharmceut. Sci. Res.* 59, 5700-5706.

[19] Zangade, S.B., Jadhav, J.D., Vibhute, Y.B., & Dawane, B.S. (2010). Synthesis and antimicrobial activity of some new chalcones and flavones containing substituted naphthalene moiety. *J. Chem. Pharm. Res. 2*(1) 310-314.

[20] Welday Kahssay, S., Hailu, G.S., & Taye Desta, K. (2021). Design, synthesis, characterization and *in vivo* antidiabetic activity evaluation of some chalcone derivatives. *Drug Des. Dev. Ther.* 15, 3119-3129.

[21] Echeverria, C., Santibañez, J.F., Donoso-Tauda, O., Escobar, C.A., & Ramirez-Tagle, R. (2009). Structural antitumoral activity relationships of synthetic chalcones. *Int. J. Mol. Sci. 10*(1) 221-231.

[22] Yadav, N., Dixit, S.K., Bhattacharya, A., Mishra, L.C., Sharma, M., Awasthi, S.K., & Bhasin, V.K. (2012). Antimalarial activity of newly synthesized chalcone derivatives *in vitro*. *Chem. Biol. Drug Des.* 80, 340-347.

[23] Sharma, N., Mohanakrishnan, D., Sharma, U.K., Kumar, R., Richa, A.K., & Sahal Sinha, D. (2014). Design, economical synthesis and antiplasmodial evaluation of vanillin derived allylated chalcones and their marked synergism with artemisinin against chloroquine resistant strains of *Plasmodium falciparum*. *Eur. J. Med. Chem.* 79, 350-368.

[24] Guantai, E.M., Ncokazi, K., Egan, T.J., Gut, J., Rosenthal, P.J., Bhampidipati, R., Kopinathan, A., Smith, P.J., & Chibale, K. (2011). Enone– and chalcone–chloroquinoline hybrid analogues: In silico guided design, synthesis, antiplasmodial activity, *in vitro* metabolism, and mechanistic studies. *J. Med. Chem. 54*(10) 3637-3649.

[25] Housecroft, C.E., & Sharpe, A.G. (2008). *Inorganic Chemistry*. 3rd ed., Pearson Prentice Hall, NJ, pp. 620-650.

[26] Bano, B., Khan, K.M., Begum, F., Lodhi, M.A., Salar, U., Khalil, R., Ul-Haq, Z., & Perveen, S. (2018). Benzylidine indane-1,3-diones: As novel urease inhibitors; synthesis, *in vitro*, and in silico studies. *Bioorg. Chem.* 81, 658-671.

[27] Szymusiak, H., Zielinski, R., Domagalska, B.W., Wilk, K.A. (2000). Electronic structure and nonlinear optical properties of model push-pull polyenes with modified indanone groups: A theoretical investigation. *Comput. Chem. 24*(3-4) 369-380.

[28] Mitka, K., Kowalski, P., Pawelec, D., & Majka, Z. (2009). Synthesis of novel indane-1,3-dione derivatives and their biological evaluation as anticoagulant agents. *Croat. Chem. Acta*, *82*(3) 613-618.

[29] Zidar, N., and Kikelj, D. (2011). Preparation and reactivity of 5-benzylidenebarbituric and 5-benzylidene-2-thiobarbituric acids. *Acta Chim. Slov. 58*(1) 151-157.

[30] Ding, S., Yao, B., Schobben, L., & Hong, Y. (2020). Barbituric acid based fluorogens: Synthesis, aggregation-induced emission, and protein fibril detection. *Molecules 25*(1) 32.

[31] Stojiljkovic, I.N., Rancic, M.P., Marinkovic, A.D.,

Cvijetic, I.N., Milcic, M.K. (2021). Assessing the potential of para-donor and para-acceptor substituted 5-benzylidenebarbituric acid derivatives as push–pull electronicsystems: Experimental and quantum chemical study. *Spectrochim. Acta A*, 253, 119576.

[32] Rabiei, Kh., & Naeimi, H. (2018). Sonocatalyzed total synthesis of N,N-diaryl-formamides through oxidation and hydrolysis reaction of gem-dichloroaziridines using DMSO/H_2O. *Curr. Org. Synth. 15*(7) 1014-1019.

[33] Niyazi, Sh., Pouramiri, B., & Rabiei, Kh. (2022). Functionalized nanoclinoptilote as a novel and green catalyst for the synthesis of Mannich bases derived from 4-hydroxy coumarin. *J. Mol. Struct. 1250* (Part B) 131908.

[34] Waghmare, A.S., and Pandit, S.S. (2017). DABCO catalyzed rapid one-pot synthesis of 1,4-dihydropyrano [2,3-*c*] pyrazole derivatives in aqueous media. *J. Saudi Chem. Soc. 21*(3) 286-290.

[35] Hu, Y., Chen, Z.C., & Le, Z.G. (2004), Organic reactions in ionic liquids: Ionic liquid promoted knoevenagel condensation of aromatic aldehydes with (2-thio)barbituric acid. *Synth. Commun. 34*(24) 4521-4529.

[36] Shirini, F., Langarudi, M.S.N., & Daneshvar, N. (2017). Preparation of a new DABCO-based ionic liquid [H_2-DABCO][H_2PO_4]$_2$ and its application in the synthesis of tetrahydrobenzo[b]pyran and pyrano[2,3-d]pyrimidinone derivatives. *J. Mol. Liq.* 234, 268-278.

[37] Theresa, L.V., Avudaiappan, G., Shaibuna, M., Hiba, K., & Sreekumar, K. (2021). A study on the physical properties of low melting mixtures and their use as catalysts/solvent in the synthesis of barbiturates. *J. Heterocycl. Chem. 58*(9) 1849-1860.

[38] Seyyedi, N., Shirini, F., & Langarudi, M.S.N. (2016). DABCO-based ionic liquids: Green and recyclable catalysts for the synthesis of barbituric and thiobarbituric acid derivatives in aqueous media. *RSC Adv.* 6, 44630-44640.

[39] Alizadeh, A., Beiranvand, Z., Safaei, Z., Khodaei, M.M., & Repo, E. (2020). Green and fast synthesis of 2-arylidene-indan-1,3-diones using a task-specific ionic liquid. *ACS Omega*, *5*(44) 28632-28636.

[40] Babu, B., Chandrasekaran, J., & Baiprabhakaran, S. (2014). Growth and characterization of hexamethylene tetramine crystals grown from solution. *Mater. Sci.-Poland*, *32*(2) 164-170.

[41] Mirjalili, B.F., Bamoniri, A., & Nezamalhosseini, S.M. (2015). BF_3/Nano-γ-Al_2O_3 Promoted knoevenagel condensation at room temperature. *J. Nanostruct. 5*(4) 367-373.

[42] Li, J.T., Dai, H.G., Liu, D., & Li, T.S. (2006). Efficient method for synthesis of the derivatives of 5-arylidene barbituric acid catalyzed by aminosulfonic acid with grinding. *Synth. Commun. 36*(6) 789-794.

[43] Wang, C., Ma, J.J., Zhou, X., Zang, X.H., Wang, Z., Gao, Y.J., & Cui, P.L. (2005). 1-n-Butyl-3-methylimmidazolium tetrafluoroborate–promoted green synthesis of 5-arylidene barbituric acids and thiobarbituric acid derivatives. *Synth. Commun. 35*(21) 2759-2764.

[44] Rathod, S.B., Gambhire, A.B., Arbad, B.R., & Lande, M.K. (2010). Synthesis, characterization and catalytic activity of $Ce_1Mg_xZr_{1-x}O_2$ (CMZO) solid heterogeneous catalyst for the synthesis of 5-arylidine barbituric acid derivatives. *Bull. Korean Chem. Soc. 31*(2) 339-343.

[45] Goli-Jolodar, O., Shirini, F., & Seddighi, M. (2016). Succinimidinium hydrogensulfate ([H-Suc]HSO_4) as an efficient ionic liquid catalyst for the synthesis of 5-arylidenepyrimidine-2,4,6(1*H*,3*H*,5*H*)-trione and pyrano-pyrimidinones derivatives. *J. Iran. Chem. Soc.* 13, 457-463.